A Space Vector Phase-Locked-Loop approach to synchrophasor, frequency and ROCOF estimation

Roberto Ferrero*, Paolo Attilio Pegoraro†, Sergio Toscani‡

*Department of Electrical Engineering and Electronics
University of Liverpool, Liverpool, United Kingdom
Email: roberto.ferrero@liverpool.ac.uk

†Department of Electrical and Electronic Engineering
University of Cagliari, Cagliari, Italy
Email: paolo.pegoraro@diee.unica.it

‡Dipartimento di Elettronica, Informazione e Bioingegneria
Politecnico di Milano, Milan, Italy
Email: sergio.toscani@polimi.it

***Abstract*—Phasor measurement units represent the most advanced measurement devices in ac power systems. Their most important feature is permitting to estimate synchrophasor, frequency and rate of change of frequency of voltages and currents in a shared, synchronized timescale. Most of the estimation algorithms have been designed to operate with a unique signal; however, ac power systems are inherently three-phase and weakly unbalanced during regular operation. Therefore, these three-phase signals benefit from peculiar properties than can be leveraged by specifically suited measurement algorithms. For this reason, space vector based techniques have been proposed. Usually, the reference frame is supposed to be stationary or rotating at the rated angular frequency. This work proposes to exploit measurements performed in a previous reporting instant in order to generate the instantaneous angular position of the reference frame, so that it tracks the phase evolution of the positive sequence synchrophasor. A P class implementation is reported, and the results highlight excellent performance. Accuracy is remarkable even under conditions going well beyond those required by compliance tests.**

***Keywords*—phasor measurement units, synchrophasor estimation, frequency measurement, voltage measurement, current measurement, power transmission, power distribution, phase locked loops, three-phase systems.**

I. Introduction

Phasor Measurement Units (PMUs) are being installed in the power transmission networks all around the world since they allow measuring synchronized phasors, frequency and Rate of Change of Frequency (ROCOF) and thus they are considered as fundamental blocks of modern wide area monitoring architectures [1]. The peculiar features of PMUs permit designing innovative network management applications, and this has stimulated, in perspective, the interest towards their employment also in distribution grids.

Dr. Pegoraro work was partially funded by Fondazione di Sardegna for the research project "SUM2GRIDS, Solutions by mUltidisciplinary approach for intelligent Monitoring and Management of power distribution GRIDS".

The synchrophasor standard (IEEE C37.118.1 [2] and its amendement [3]) defines the signals, the accuracy indexes and the corresponding limits for evaluating the performances of PMU algotirhms both under steady-state and dynamic conditions. The underlying idea is to translate requirements that allow covering different application fields in terms of simple tests. On the one hand, PMU designs have to cope with the wide range of operating scenarios that may occur in power systems; on the other hand, fast dynamics and robustenss to disturbances are conflicting requirements that have to be carefully balanced according to the purpose. For this reason, [2] introduces two performance classes. P class is devoted to relaying applications, thus requiring fast response and low latency. M class, favoring high accuracy, is intended for measurement applications.

The importance of PMUs in power systems has triggered the research towards different aspects of their design, and in particular on the implemented algorithms that play a fundamental role in performance. In this respect, many proposals have emerged in the last decade (see [4] for a review) as far as synchrophasor, frequency and ROCOF estimation techniques are concerned. Different approaches have been employed: discrete fourier transform (DFT) [2], interpolated DFT (IpDFT) [5], iterative IpDFT [6], compressive sensing on DFT [7], cascade boxcar filtering [8], dual channel design for simultaneous class P and M compliance [9].

Recently, techniques that leverage the three-phase characteristics of electrical signals to improve the effectiveness of estimation algorithms have been proposed by the authors of this work [10]. In [11], positive sequence synchrophasor, frequency and ROCOF measurements are obtained by computing the space vector (SV) in a reference frame that rotates at the rated angular frequency and by filtering its magnitude and phase angle with FIR filters (including first and second order differentiators). In [12], the SV is used as a complex input to the IpDFT algorithm. Estimation is improved thanks to the considerably lower amplitude of the image component.

Similarly [13] proposes to use Taylor-Fourier filters on the SV computed in a stationary reference frame, with remarkable advantages in terms of computational burden.

SV based techniques have been proposed also by other researchers; for example, in [14] the SV transformation on a stationary reference frame is used to compute the positive sequence synchrophasor. In [15] the positive sequence synchrophasor is instead measured by means of three-phase demodulation in a rotating reference frame.

Another significant approach used to deal with off-nominal frequency conditions and slow phase modulations is represented by frequency-tracking [8], [9], where feedback allows a continuous tuning of the procedure by following frequency variations. Phase locked loops (PLLs) can be used to measure synchrophasor [16], frequency [17] or to increase the performance of PMU algorithms based on Taylor-Fourier filters [18].

In this paper, a digital PLL is employed in order to enhance the accuracy of SV-based estimation algorithms [11]. The basic idea is to employ measurements in the preceding reporting instant to construct the instantaneous position of a rotating reference frame. The SV transormation is performed on this reference frame while positive sequence synchrophasor, freqeuncy and ROCOF estimates are obtained by filtering its magnitude and phase. Continuous phase tracking allows using filters having narrower passband without suffering from significant scalloping loss. In turns, this results in a more effective compromise between disturbance rejection and measurement bandwith. Two different P-class compliant implementations are presented and their performances are evaluated by applying test signals going beyond the requirements of the IEEE synchrophasor standard.

II. Dynamic synchrophasor and SV approach

Dynamic performance tests for PMUs were firstly introduced by the 2011 revision of the IEEE synchrophasor standard [2]. The underlying concept is that a typical electrical signal $x(t)$ in an ac power system can be modeled as a sine wave at the rated frequency f_0 modulated both in magnitude and phase; an unwanted term $d(t)$ containing harmonic and non-harmonic disturbances may be present. In terms of equations:

$$x(t) = \sqrt{2}X(t)\cos(\omega_0 t + \varphi(t)) + d(t) \tag{1}$$

where $\omega_0 = 2\pi f_0$. The target of PMU techniques is to estimate $X(t)$ and $\varphi(t)$ as well as its first and second order derivatives (thus allowing frequency and ROCOF measurements) referred to to the coordinated universal time scale (UTC). $\bar{X}_S(t) = X(t)e^{j\varphi(t)}$ is the dynamic synchrophasor associated with the signal $x(t)$. The challenge that estimation techniques have to face is ensuring extended measurement bandwidth together with high disturbance rejection; several proposals can be found in the literature. Considering sinusoidal steady-state operation at the frequency f (and rated angular frequency ω) characterized by the phasor $\bar{X}$, the time-domain signal can be written as:

$$x(t) = \frac{1}{\sqrt{2}}\left[\bar{X}e^{j(\omega-\omega_0))} + \bar{X}^* e^{-j(\omega+\omega_0))}\right] \tag{2}$$

where * denotes the complex conjugate operator. Recalling the signal model (1), the synchrophasor is $\bar{X}_S(t) = \bar{X}(t)e^{j(\omega-\omega_0)t}$. It should be noticed that if the synchrophasor is obtained by filtering, the negative frequency image component acts as a large disturbance which has to be suppressed.

Many applications only require estimating the positive sequence synchrophasor, as well as frequency and its rate of change. In this case, SV based techniques are extremely attractive, since they exploit the three-phase peculiarities of electrical quantities. Furthermore, the computation of *per-phase* synchrophasors is avoided, with clear advantages in terms of computational burden. A generic three-phase signal can be written using a compact vector form as follows:

$$\boldsymbol{x}_{abc}(t) = \begin{bmatrix} x_a(t) \\ x_b(t) \\ x_c(t) \end{bmatrix} \tag{3}$$

where $x_p(t)$ ($p \in \{a, b, c\}$) is the phase p signal that can be decomposed as in (1).

SV-based techniques require applying the SV transformation to the three-phase samples. A UTC synchronized rotating reference frame is considered, and the complex-valued SV signal $\bar{x}_{SV}$ is obtained:

$$\begin{aligned}\bar{x}_{SV}(t) &= \\ &= \sqrt{\frac{2}{3}}\begin{bmatrix} 1 & \bar{\alpha} & \bar{\alpha}^2 \end{bmatrix}\boldsymbol{x}_{abc}(t)\, e^{-j\beta(t)}\end{aligned} \tag{4}$$

where $\bar{\alpha} = e^{j2\pi/3}$ while $\beta(t)$ represents the instantaneous angular position of the rotating reference frame. In [10] and [11] $\beta(t) = \omega_0 t$ was considered. Remembering that power systems are weakly unbalanced, the SV signal can be written as:

$$\bar{x}_{SV}(t) = \bar{X}_{+,S}(t) + \bar{d}_{SV}(t) \tag{5}$$

$\bar{X}_{+,S}$ is the positive sequence synchrophasor, while $\bar{d}_{SV}(t)$ is a complex disturbance due to harmonic, non-harmonic components and unbalance. It is particularly interesting to obtain the expression of the SV under sinusoidal steady-state conditions characterized by the symmetrical components $\bar{X}_+, \bar{X}_-, \bar{X}_0$ and the frequency f (or the corresponding angular frequency ω). Under these assumptions:

$$\bar{x}_{SV}(t) = \bar{X}_+ e^{j(\omega-\omega_0)t} + \bar{X}_-^* e^{-j(\omega+\omega_0)t} \tag{6}$$

In this case, the positive sequence synchrophasor results $\bar{X}_{+,S} = \bar{X}_+ e^{j(\omega-\omega_0)t}$. The zero sequence term does not affect the synchrophasor estimate, while the negative sequence component plays the role of disturbance.

It should be noticed that (6) is similar to (2), but the negative frequency component is considerably smaller in this case thanks to the *quasi* three-phase symmetry. This makes the synchrophasor estimation considerably easier.

The SV algorithm presented in [11] exploits the demodulation effect of the rotating reference frame. The positive sequence term results in slowly changing real and imaginary parts (thus also magnitude and phase), therefore it can be extracted by proper filters as shown in Fig. 1; estimated quantities are denoted with the subscript e.

A first filter H is applied to the real and imaginary parts of the SV signal; it allows removing most part of disturbances.

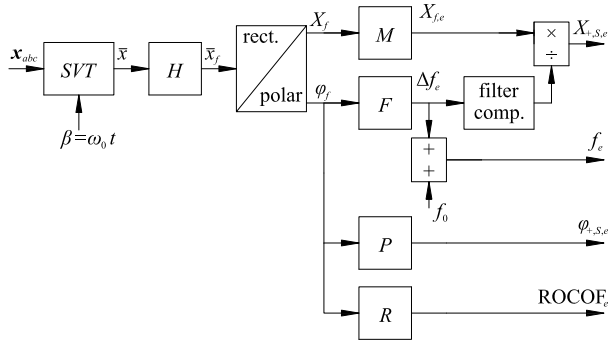

Fig. 1. Block diagram of SV-based PMU algorithms

Then, two FIR filters (M and P) are applied to the magnitude and phase of the resulting signal. First and second order limited-band FIR differentiators are used to extract frequency and ROCOF from the phase angle. For improved accuracy, the frequency estimate is used to compensate for scalloping loss due to the input filter H; group delay produced by digital filters has also to be properly managed. Details about filters, design equations and achievable performance can be found in [11].

III. Proposed Algorithm

The vast majority of PMU techniques are based on FIR filtering: therefore, for each reporting instant they estimate synchrophasor, frequency and ROCOF starting from N samples of an elecrical signal. Group delay due to the algorithms is considered during time stamping. In many cases, as in the reference algorithms reported in [2], [3], the first operation to be carried out is quadrature demodulation of the N acquired samples by means of sinewaves at the rated frequency f_0. The sampling frequency f_s (and the corresponding period T_s) is typically chosen as an integer multiple of the rated frequency, thus $f_s = Mf_0$, $M \in \mathbb{N}$. In this way, the two quadrature sinewaves can be stored in M-row lookup tables instead of continuously computing trigonometric functions.

As far as SV-based algorithm, the minimum length of the observation window that allows performing a measurement depends on N_H, namely the number of taps of filter H, and N_{max}, which is the number of taps of the longest filter between M, P, F and R; in particular, $N = N_H + N_{max} - 1$. Let us suppose that N is an odd number and that filters are designed to introduce a constant group delay corresponding to an integer number of samples $L = (N-1)/2$.

A reference frame rotating at the rated angular speed is generally employed in SV-based algorithms, since, as explained before, it results in lower computational burden. It should be noticed that measurements in a reporting instant can be exploited to forecast the synchrophasor phase during the N-sample observation window required for the next estimation. Under typical operating conditions, this prediction is fairly good: the evolution of the phase angle is smooth and furthermore, when a small reporting period T_{RR} is employed, the observation windows of consecutive measurements are largely overlapped, being NT_S considerably higher than T_{RR}. In turns, this phase forecast can be used to generate the instantaneous position of the rotating reference frame, thus enabling a more effective baseband demodulation.

A first possibility is to obtain β by exploiting the preceding phase, frequency and ROCOF estimates. In this case, for $k, n \in \mathbb{N}$, $-L \le n \le L$:

$$\begin{aligned}\beta(kT_{RR}+nT_s) = \varphi_{+,S,e}((k-1)T_{RR}) + \\ + 2\pi f_e((k-1)T_{RR})\,(T_{RR}+nT_s) + \\ + \pi \mathrm{ROCOF}_e((k-1)T_{RR})\,(T_{RR}+nT_s)^2\end{aligned} \tag{7}$$

where $\varphi_{+,S,e}((k-1)T_{RR})$, $f_e((k-1)T_{RR})\,(T_{RR}+nT_s)$ and $\mathrm{ROCOF}_e((k-1)T_{RR})\,(T_{RR}+nT_s)^2$ are, respectively, the estimations of the positive sequence synchrophasor phase angle, of the frequency and of the ROCOF in the last reporting instant. It is also useful to write the expression of the corresponding angular speed:

$$\begin{aligned}\dot{\beta}(kT_{RR}+nT_s) = 2\pi f_e((k-1)T_{RR}) + \\ + 2\pi \mathrm{ROCOF}_e((k-1)T_{RR})\,(T_{RR}+nT_s)\end{aligned} \tag{8}$$

ROCOF estimation is known to be particularly sensitive to measurement noise and disturbances. Therefore, it is worth investigating the employment of a first order expansion to compute β:

$$\begin{aligned}\beta(kT_{RR}+nT_s) = \varphi_{+,S,e}((k-1)T_{RR}) + \\ + 2\pi f_e((k-1)T_{RR})\,(T_{RR}+nT_s)\end{aligned} \tag{9}$$

After having obtained the instantaneous position of the reference frame, the SV signal can be computed as in (4); filters H, M, P, F and R can be used as before. Thanks to phase tracking, scalloping loss is expected to be negligible, thus there is no need to compensate for it. For the same reason, filters with narrower bandwidths can be favourably employed, since they permit better disturbance rejection without sacrificing accuracy.

It should be noticed that, as from the synchrophasor standard, phase should be measured with respect to a reference frame rotating at the rated angular frequency ω_0. On the contrary, frequency is defined in a stationary reference frame, while ROCOF has to be evaluated in a reference frame having constant angular speed. Therefore, assuming that β is computed with a second order expansion, introducing $\Delta\varphi_{+,S,e}$, Δf_e and $\Delta\mathrm{ROCOF}_e$ as the outputs of filter P, F and R, respectively, positive sequence synchrophasor phase, frequency and ROCOF can be obtained as follows:

$$\begin{aligned}\varphi_{+,S,e}(kT_{RR}) = \Delta\varphi_{+,S,e}(kT_{RR}) + \beta(kT_{RR}) \\ - \omega_0 kT_{RR} - \theta_0\end{aligned} \tag{10}$$

$$f_e(kT_{RR}) = \Delta f_e(kT_{RR}) + \frac{1}{2\pi}\dot{\beta}(kT_{RR}) \tag{11}$$

$$\begin{aligned}\mathrm{ROCOF}_e(kT_{RR}) = \Delta\mathrm{ROCOF}_e(kT_{RR}) \\ + \mathrm{ROCOF}_e((k-1)T_{RR})\end{aligned} \tag{12}$$

θ_0 depends on the reference frame which has been employed to measure phase angles. The corresponding expressions to be used when β is obtained with a first order expansion can be derived straightforwardly.

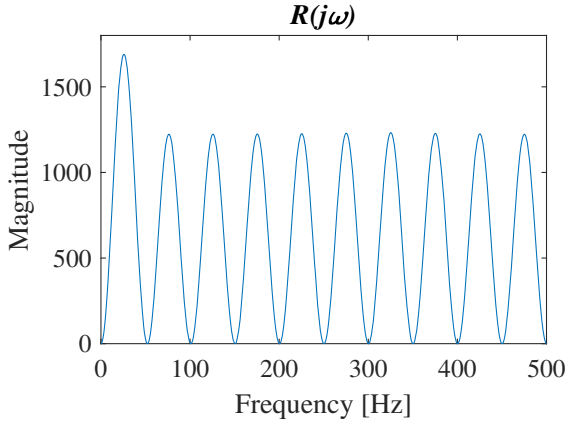

Fig. 2. Magnitude response of filter R

IV. Algorithm implementation

The proposed SV-based phase-tracking technique is particularly interesting as far as class P compliance has to be met. If constant group delay FIR filters are employed, their overall length has to be lower than four nominal power cycles because of latency constraints [3]. Phase modulation tests have to be carried out with modulation frequencies up to 2 Hz (50 Hz rated frequency and 50 phasors/s reporting rate are assumed). This means that the phase evolution has to be followed over a time window which is shorter than $4/25$ of a modulation period. Furthermore, measurements in the previous reporting instant are employed to forecast the phase for no more than $1/25$ of a modulation period.

A class P compliant PMU algorithm has been implemented by exploiting the previously presented approach; as in the previous paragraph, f_0=50 Hz rated frequency and 50 phasors/s reporting rate are assumed. 10 kHz sampling frequency has been employed, while a target latency of L=300 samples (thus corresponding to 1.5 nominal cycles) has been considered. As an additional constraint, the algorithm is required to comply with P class limits for harmonic disturbances even when frequency deviates up to 1 Hz with respect to its rated value. Both first and second order frequency tracking have been considered and compared.

Designing the filters represents the trickiest task, since their responses heavily affect overall performance. Constant group delay FIR filters are assumed, thus the maximum latency translates in 601 coefficients for the cascade between the input filter H and those employed for magnitude, phase, frequency and ROCOF estimations. This means that the sum between the number of coefficients of the input filter and the highest among the others has to be equal to 602. Since ROCOF estimation is particularly sensitive to harmonic disturbance, 401 coefficients have been allocated for the design of the second order, partial band differentiator R. In this way, an equiripple filter having zeros in the multiples of f_0 has been obtained; its magnitude response is shown in Fig. 2.

Coefficients are scaled in order to provide zero error when estimating the second derivative of a parabolic input, thus corresponding to a linearly increasing deviation between frequency and rotational speed of the reference frame. It should be noticed that the derivative of the magnitude response is zero at multiples of f_0; this allows achieving good harmonic disturbance rejection even under off-nominal frequency conditions.

Filter F has been designed as a 401-tap equiripple partial-band differentiator; since a very narrow bandwidth is required, it is possible to obtain good stopband attenuation. Coefficients are scaled so that zero error is achieved when estimating the slope of a ramp, which occurs in case of constant slip between space vector and reference frame. Filters M and P, used for magnitude and phase estimations, share the same design parameters, being them equiripple low-pass filters having 2-Hz passband edge, 50-Hz stopband edge and 10^{-3} passband ripple.

Thanks to frequency tracking, bandwidth of filter H is not critical; in order to further improve harmonic disturbance rejection, a 201 coefficient boxcar filter has been chosen.

V. Tests and results

The test signals prescribed by the synchrophasor standard [2] for P-class compliance verification have been considered for the simulation tests together with additional test conditions. The performance of the proposed algorithms have been assessed using total vector error (TVE), absolute frequency error (FE) and absolute ROCOF error (RFE) as indicators. In the following, $f_0 = 50\,\text{Hz}$, the initial phase-angle of phase a is zero and the positive-sequence amplitude is $X_+ = 1\,\text{p.u.}$; test duration is 1 s.

The first set of tests has been performed under off-nominal frequency conditions ($f \in [48, 52]\,\text{Hz}$). Thanks to the frequency-locked reference frame, TVE and FE values are negligible and due to numerical noise ($< 10^{-11}\,\%$ and $< 10^{-10}$mHz, respectively). There is no noticeable difference when β is obtained with first and second order expansions; since ROCOF is constant, no disturbances are present and so its estimate is virtually error-free. When additive white gaussian noise (AWGN) is superimposed with signal-to-noise ratio (SNR) of 60 dB, performance degrades but errors are still fairly low. TVE is below $1.2 \cdot 10^{-2}\,\%$ for both phase tracking strategies, while maximum FE is about 1 mHz. The difference between the two approaches is very small, since RFE always remains below $0.1\,\text{Hz/s}$.

A second set of tests in presence of harmonic disturbances has been performed. A single harmonic having amplitude equal to $1\,\%$ of the fundamental has been added; different harmonic orders (up to the 50th) have been considered. Under nominal frequency operation, errors are very small (TVE $< 1.7 \cdot 10^{-4}\,\%$, FE $< 0.073\,\text{mHz}$ and FE $< 0.0014\,\text{Hz/s}$) and almost identical for first and second order implementations. Like previous tests, the presence of additional noise leads to higher errors (e.g. maximum TVE of about $10^{-2}\,\%$ for all the considered harmonic orders), which are mostly due to the equivalent noise bandwidths of the filters.

When fundamental frequency is changed to $51\,\text{Hz}$, (not required by compliance tests) different aspects emerge. Fig. 3 shows the maximum RFE as a function of the order of the harmonic disturbance (dotted line represents the P class limit). It is clear that, when off-nominal condition occurs, the zeros of filters H and R no longer result in perfect cancellation of the harmonics. Then, RFE value strictly depends on the shape of

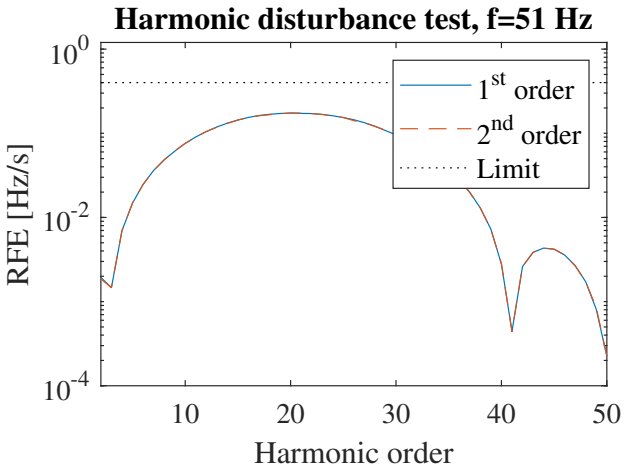

Fig. 3. Maximum RFE for a 51 Hz signal with a single 1% additional harmonic.

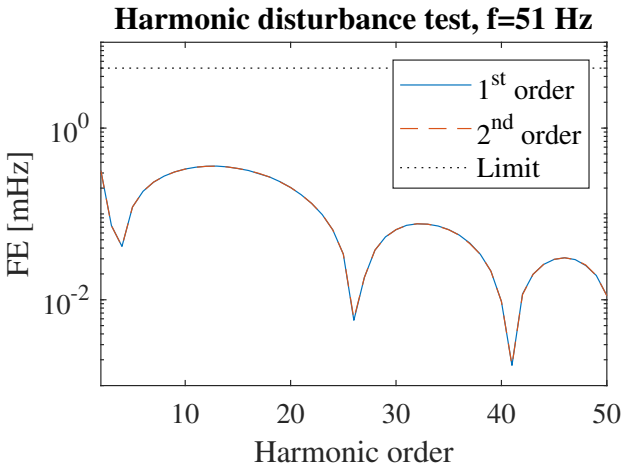

Fig. 4. Maximum FE for a 51 Hz signal with a single 1% additional harmonic.

the filters and, thus, on the harmonic order of the disturbance, as reported in the figure. First and second order ROCOF estimations are almost the same, resulting in maximum RFE values slightly above 0.17 Hz/s. Similar considerations hold also for FE which, as shown in Fig. 4, remains below 0.36 Hz. Nonzero RFE values suggest that the two PLL implementations should achieve different results in terms of TVE. This is confirmed by Fig. 5, where differences between the two approaches are evident for harmonic orders corresponding to higher RFEs. In this case, TVE is reduced by almost an order of magnitude, even though it is not immediately evident because of the logarithmic scale. However, it should be noticed that when AWGN at 60 dB SNR is added, TVE values become almost the same as previously evaluated during off-nominal tests; this denotes that the effect of noise is largely prevailing. It is important to recall that the adopted SNR is fairly conservative and chosen in order to stress the algorithms: higher SNRs can be easily achieved with proper acquisition stages.

Finally, tests under phase-angle modulation (PM) have been performed. PM signals with sinusoidal modulation have

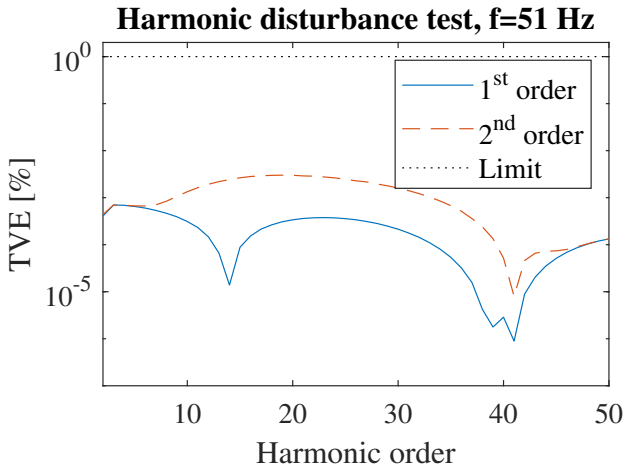

Fig. 5. Maximum TVE for a 51 Hz signal with a single 1% additional harmonic.

the following expression:

$$x_p(nT_s) = X_p \cos\left(2\pi f_0 n T_s + \psi_p + k_a \cos\left(2\pi f_m n T_s - \pi\right)\right) \tag{13}$$

where $p \in \{a, b, c\}$, and ψ_p is $0, -\frac{2}{3}\pi, +\frac{2}{3}\pi$ depending on the considered phase; f_m represents the modulation frequency. These signals are useful to test the tracking capabilities of the algorithms, since frequency and ROCOF are time-dependent quantities (cosinusoidal functions of time). Figures 6, 7 and 8 report, respectively, the maximum TVE, FE and RFE obtained by varying $f_m \in (0, 2]$. Fig. 6 shows that first and second order PLL strategies have different accuracies. Estimation errors are due to the passband characteristics of the filters and to the accuracy of baseband demodulation. As expected, the worst TVE values are achieved at the highest f_m. Figure 8 shows that the largest RFE 0.019 Hz/s corresponds to the highest difference between synchrophasor estimations obtained with first and second order approaches in Fig. 6 (maximum difference 0.0349 % with $f_m = 2$ Hz[1]). In the presence of AWGN, the TVEs are higher but similar differences between first and second order implementations can be found. PM tests have also been performed by changing the fundamental frequency and the performances are virtually the same as in the nominal frequency case thanks to the phase locking capabilities of the algorithms.

VI. Conclusions

The paper discusses the employment of digital PLL techniques to enhance SV-based algorithms for estimating synchrophasor, frequency and ROCOF in PMU applications. Simulation tests, performed under different conditions, show that PLL allows remarkable estimation accuracy when off-nominal frequency conditions occur. Results denote the lowest errors of the second order PLL implementation under PM conditions, but they also highlight how a first order PLL is usually sufficient to cope with the typical dynamics of electric signals.

[1] this TVE difference is comparable with the contribution due to the typical synchronization error of a PMU.

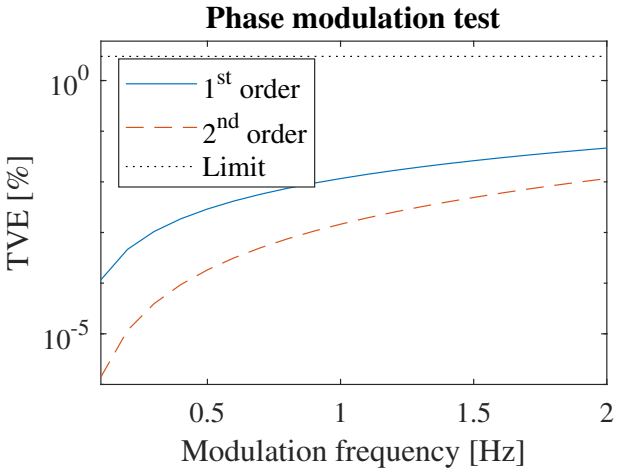

Fig. 6. Maximum TVE for phase-modulated signals.

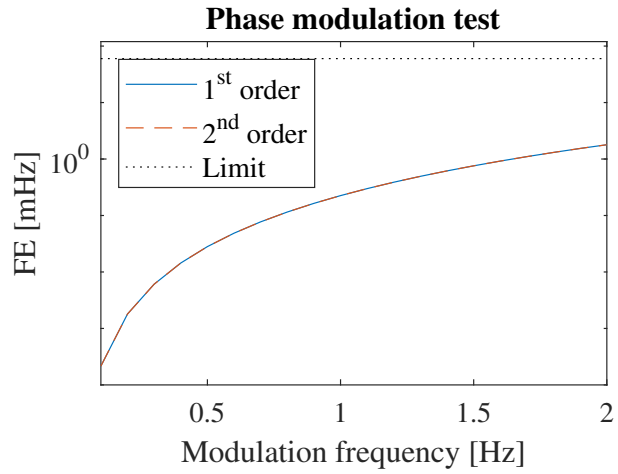

Fig. 7. Maximum FE for phase-modulated signals.

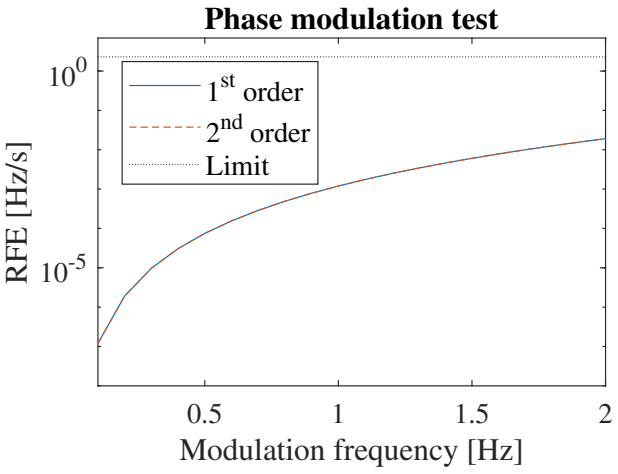

Fig. 8. Maximum RFE for phase-modulated signals.

REFERENCES

[1] AA. VV., *Phasor Measurement Units and Wide Area Monitoring Systems*, 1st ed., A. Monti, C. Muscas, and F. Ponci, Eds. Academic Press, 2016.

[2] *IEEE Standard for Synchrophasor Measurements for Power Systems*, IEEE IEEE Std C37.118.1-2011 (Revision of IEEE Std C37.118-2005), Dec. 2011.

[3] *IEEE Standard for Synchrophasor Measurements for Power Systems – Amendment 1: Modification of Selected Performance Requirements*, IEEE IEEE Std C37.118.1a-2014 (Amendment to IEEE Std C37.118.1-2011), Apr. 2014.

[4] C. Muscas and P. A. Pegoraro, "Algorithms for synchrophasors, frequency, and rocof," in *Phasor Measurement Units and Wide Area Monitoring Systems*, 1st ed., A. Monti, C. Muscas, and F. Ponci, Eds. Elsevier, Academic Press, 2016, ch. 3, pp. 21–51.

[5] D. Belega and D. Petri, "Accuracy analysis of the multicycle synchrophasor estimator provided by the interpolated DFT algorithm," *IEEE Trans. Instrum. Meas.*, vol. 62, no. 5, pp. 942–953, May 2013.

[6] A. Dervikadi, P. Romano, and M. Paolone, "Iterative-interpolated dft for synchrophasor estimation: A single algorithm for p- and m-class compliant pmus," *IEEE Trans. Instrum. Meas.*, vol. 67, no. 3, pp. 547–558, Mar. 2018.

[7] M. Bertocco, G. Frigo, C. Narduzzi, and F. Tramarin, "Resolution enhancement by compressive sensing in power quality and phasor measurement," *IEEE Trans. Instrum. Meas.*, vol. 63, no. 10, pp. 2358–2367, Oct. 2014.

[8] A. Roscoe, "Exploring the relative performance of frequency-tracking and fixed-filter phasor measurement unit algorithms under C37.118 test procedures, the effects of interharmonics, and initial attempts at merging p-class response with m-class filtering," *IEEE Trans. Instrum. Meas.*, vol. 62, no. 8, pp. 2140–2153, Aug. 2013.

[9] P. Castello, J. Liu, C. Muscas, P. A. Pegoraro, F. Ponci, and A. Monti, "A fast and accurate PMU algorithm for P+M class measurement of synchrophasor and frequency," *IEEE Trans. Instrum. Meas.*, vol. 63, no. 12, pp. 2837–2845, Dec. 2014.

[10] S. Toscani and C. Muscas, "A space vector based approach for synchrophasor measurement," in *Instrum. and Meas. Technol. Conf. (I2MTC) Proc., 2014 IEEE Int.*, May 2014, pp. 257–261.

[11] S. Toscani, C. Muscas, and P. A. Pegoraro, "Design and performance prediction of space vector-based pmu algorithms," *IEEE Trans. Instrum. Meas.*, vol. 66, no. 3, pp. 394–404, Mar. 2017.

[12] R. Ferrero, P. A. Pegoraro, and S. Toscani, "Employment of interpolated DFT-based pmu algorithms in three-phase systems," in *IEEE AMPS*, Liverpool, UK, Sep. 2017.

[13] P. Castello, R. Ferrero, P. A. Pegoraro, and S. Toscani, "Synchrophasor and frequency estimations: Combining space vector and taylor-fourier approaches," in *Instrum. and Meas. Technol. Conf. (I2MTC) Proc., 2018 IEEE Int.*, May 2018, pp. 1–6.

[14] L. Zhan, Y. Liu, and Y. Liu, "A Clarke transformation-based DFT phasor and frequency algorithm for wide frequency range," *IEEE Trans. Smart Grid*, vol. 9, no. 1, pp. 67–77, Jan. 2018.

[15] F. Messina, P. Marchi, L. R. Vega, C. G. Galarza, and H. Laiz, "A novel modular positive-sequence synchrophasor estimation algorithm for pmus," *IEEE Trans. Instrum. Meas.*, vol. 66, no. 6, pp. 1164–1175, June 2017.

[16] M. Karimi-Ghartemani, B.-T. Ooi, and A. Bakhshai, "Application of enhanced phase-locked loop system to the computation of synchrophasors," *IEEE Trans. Power Del.*, vol. 26, no. 1, pp. 22–32, Jan. 2011.

[17] A. Carboni and A. Ferrero, "A Fourier transform-based frequency estimation algorithm," *IEEE Trans. Instrum. Meas.*, vol. 67, no. 7, pp. 1722–1728, Jul. 2018.

[18] J. de Serna, "Synchrophasor measurement with polynomial phase-locked-loop Taylor-Fourier filters," *IEEE Trans. Instrum. Meas.*, vol. 64, no. 2, pp. 328–337, Feb. 2015.